NJC

PAPER

Cite this: *New J. Chem.*, 2018, **42**, 14827

Using theoretical calculations to predict the redox potential of mononuclear manganese complexes†

Juan L. Puzzolo, [a] Salvador I. Drusin, [bc] Verónica A. Daier, [ad] Sandra Signorella [ad] and Diego M. Moreno *[ad]

Received 29th June 2018,
Accepted 2nd August 2018

DOI: 10.1039/c8nj03254h

rsc.li/njc

The rational design of biomimetic complexes of metalloenzymes involved in redox processes is of great interest in bioinorganic chemistry. Its purpose is to utilize the redox properties of mimics and use them as redox-active catalysts. To obtain efficient artificial catalysts, it is necessary to model structurally and electronically the active site of the enzymes. In particular, for redox catalysis, it is necessary that the biomimetic complexes achieve a certain redox potential so their prediction is a valuable tool to improve the rational design of catalysts with specific properties. In this work we set out to predict the one electron redox potential for a series of mononuclear Mn models of Mn superoxide dismutase enzymes using density functional calculations of low computational cost. We obtained an excellent linear correlation between calculated and experimental redox potentials referenced against the ferrocene/ferrocenium (Fc/Fc^{+}) couple, when solvation effects were included. Additionally, we validated the strategy predicting the redox potentials of two complexes synthesized in our laboratory.

Introduction

Numerous biological reactions are catalyzed by metalloenzymes that exploit the redox properties of their metal site.[1] Among them manganese superoxide dismutase (MnSOD) enzymes catalyze the dismutation of a superoxide radical into oxygen and hydrogen peroxide according to Scheme 1 using a redox cycle Mn(II)/Mn(III). MnSOD is essential in eukaryotic cells since it is located in the mitochondria of aerobic organisms.[2]

The active site of MnSOD is formed by the Mn ion in a distorted trigonal bipyramidal environment, N_3O_2, generated by coordination with three histidine and one aspartate residue, and one OH^- or H_2O molecule. This particular environment establishes the redox potential of the Mn ion at 8 mV (*vs.* Ag/AgCl KCl 0.1 M).[3]

There are numerous pathologies and cellular processes that cause MnSOD inactivation, which disrupts the redox homeostasis in the cell. The treatment with the native enzyme gives rise to a variety of immunological problems due to the nonhuman origin of the enzyme, thus, the use of alternative therapeutic agents is needed.[4] This has led to great interest in the development of functional biomimetic models of MnSOD. The aim is to find complexes that are easy to synthesize with structural and electronic features which can be easily modified, in order to modulate their catalytic activity. Considering this, these types of complexes can also be used to catalyze reactions in fine chemistry and industrial processes.[5,6]

$$Mn^{3+} + O_2^{\cdot -} \longrightarrow Mn^{2+} + O_2$$

$$Mn^{2+} + 2H^{+} + O_2^{\cdot -} \longrightarrow Mn^{3+} + H_2O_2$$

Scheme 1 Redox cycle of MnSOD.

Many manganese mononuclear complexes have been reported to have SOD activity, which can be classified according to the ligand type: macrocyclic, Schiff's base, porphyrin, corrole derivatives, acyclic multidentate, or peptide based-ligands.[7–13] It is important that these biomimetic complexes have a redox potential similar to the natural enzyme so that the redox process associated with catalytic activity can take place.[3]

Schiff bases, or imines, have long been known to be useful metal ligands,[14,15] where salpn = 1,3-bis(salicylidenamino)propane has been studied in detail.[16,17] This type of ligand makes it possible to modify the electronic features of the complexes by inserting different substituents in their aromatic rings (Fig. 1). The redox potential of the complexes can be adjusted through these modifications. Therefore, the ability to adjust the redox potential allows control of the catalytic activity.

[a] *Instituto de Química Rosario (IQUIR, CONICET-UNR), Suipacha 570, Rosario S2002LRK, Santa Fe, Argentina. E-mail: moreno@iquir-conicet.gov.ar*
[b] *Instituto de Biología Molecular y Celular de Rosario (IBR, CONICET-UNR), Ocampo y Esmeralda, predio CCT, Rosario 2000, Argentina*
[c] *Área Física, Facultad de Ciencias Bioquímicas y Farmacéuticas, Universidad Nacional de Rosario, Rosario S2002LRK, Argentina*
[d] *Área Química General e Inorgánica, Facultad de Ciencias Bioquímicas y Farmacéuticas, Universidad Nacional de Rosario, Rosario S2002LRK, Argentina*

† Electronic supplementary information (ESI) available. See DOI: 10.1039/c8nj03254h

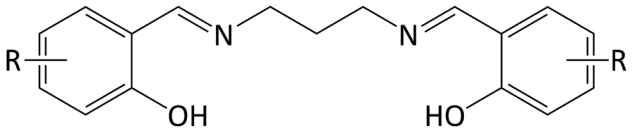

Fig. 1 Schematic representation of the Schiff base ligand used in this work.

Computational methods have become a valuable tool for describing the electronic properties of biomimetic complexes.[18,19] One of the applications of these methods in modern chemistry is the prediction of the redox potentials of chemical species such as metal complexes.[20–22]

In this work, a low computational cost model based in the thermodynamic cycle shown in Scheme 2 was applied to obtain the redox potentials of a series of manganese complexes of salpn ligand derivatives (Fig. 1 and 2) using density functional calculations and the free energy change of the half reaction. The results were compared with those reported in the literature and we obtained a linear correlation that allowed us to predict with great accuracy the redox potential of two complexes synthesized in our laboratory.

Theoretical and computational details

All calculations were performed using the hybrid B3LYP[23] functional as implemented in the Gaussian 09 package.[24] This functional was used successfully in theoretical studies that involved manganese complexes.[25–28] In this work we have employed the 6-31G** basis set for the first-row to the third-row atoms and LANL2DZ ECP for Mn and Br atoms.[29,30] The solvent effects were computed by the polarizable continuum model (PCM)[31] and the continuum solvation model SMD[32] with the dimethylformamide DMF dielectric constant. All the optimized structures are proved to be local minima using frequency calculations.

Using the thermodynamic cycle depicted in Scheme 2, we obtained the calculated redox potential of a family of Mn complexes derived from the 1,3-bis(salicilidenamine)propane ligand (salpn). First, the structure optimization under vacuum of each complex at the two redox states was performed, and then the free energy in solution ($G_{(soln)}$) of these ones was calculated by geometry optimization and frequency calculations. The analytical

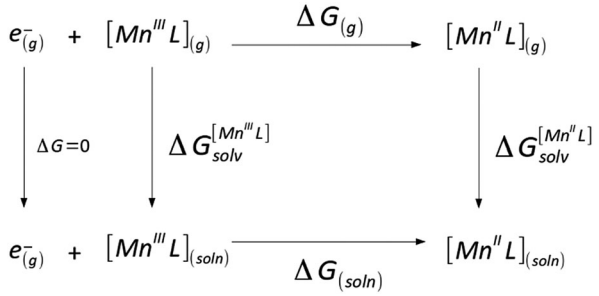

Scheme 2

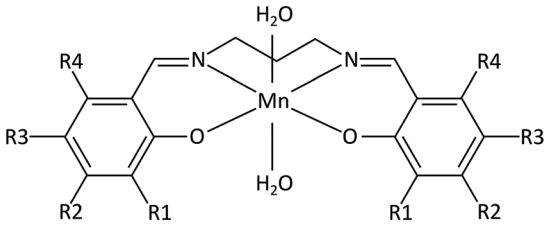

	R1	R2	R3	R4
Complex-1	H	OMe	H	OMe
Complex-2	OEt	H	H	H
Complex-3	H	H	Cl	H
Complex-4	OMe	H	Br	H
Complex-5	Br	H	Cl	H
Complex-6	H	H	NO_2	H
Complex-7	Br	H	NO_2	H

Fig. 2 The series of mononuclear Mn complexes derived from the X-salpn ligand used in this work.

vibrational frequencies required to compute the $G_{(soln)}$ value were obtained by frequency calculations over local minima structures of each complex in solution. These structures were optimized using the self-consistent reaction field (SCRF) approach, with the dielectric constant of DMF, starting from the gas-phase local minima structure. All these methods were used as they are implemented in the Gaussian 09 package by default. These data were employed to obtain the calculated redox potential (E^0_{calc}) using the eqn (1) and (2).

$$\Delta G_{(soln)} = G^{[Mn^{II}L]}_{(soln)} - G^{[Mn^{III}L]}_{(soln)} \quad (1)$$

$$E^0_{calc} = -\frac{\Delta G_{(soln)}}{nF} \quad (2)$$

Complexes studied: model building

The complexes studied in this work are summarized in Fig. 2 and the experimental redox potentials were taken from the literature.[17] This series of complexes was used to build the model system.

Validation complexes

Two complexes (8 and 9) previously synthesized by our group were used in order to validate the applied strategy.[33] Complex-8 is the difluoro-substituted (R1 = R3 = F) and complex-9 is the dichloro-substituted derivative (R1 = R3 = Cl).

Results and discussion

A family of mononuclear manganese complexes derived from the salpn ligand and their phenyl substituted derivatives was selected to perform our studies. These complexes have been correctly characterized in the literature and their catalytic activities have been reported.[17]

Structural and electronic properties

Geometry optimizations were performed considering the effects of the DMF solvent using two models, PCM and SMD,

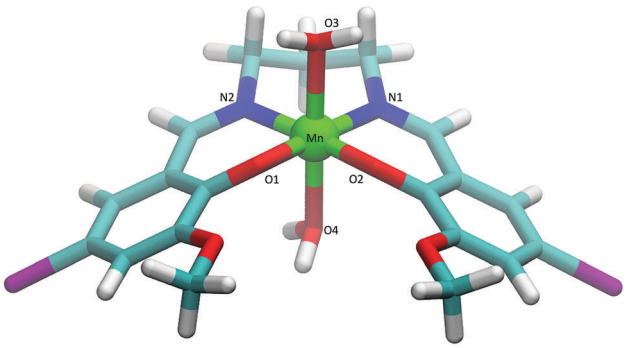

Fig. 3 Optimized structure of complex 4. Carbon atoms are shown in cyan, nitrogen atoms are shown in blue, manganese atoms are shown in green, oxygen atoms are shown in red and bromine atoms are shown in purple.

Table 1 Relevant geometrical parameters of the crystal[17] and optimized structures of complex-4 with PCM as the solvent model

Distance (Å)	Crystal structure	Optimized structure	Angles (°)	Crystal structure	Optimized structure
Mn–O1	1.863	1.88	O1–Mn–O2	86.5	89.4
Mn–O2	1.868	1.87	O1–Mn–O3	89.8	92.4
Mn–O3	2.275	2.29	O1–Mn–O4	93.3	92.0
Mn–O4	2.203	2.33	O1–Mn–N1	176.5	178.0
Mn–N1	2.026	2.05	O1–Mn–N2	90.6	88.3
Mn–N2	2.017	2.05	O2–Mn–O3	91.2	94.1
Angles (°)			O2–Mn–O4	90.5	88.6
N1–Mn–N2	91.8	93.6	O2–Mn–N1	91.1	88.7
N2–Mn–O3	87.8	88.2	O2–Mn–N2	177.0	176.7
N2–Mn–O4	90.5	89.2	N1–Mn–O3	87.7	88.2
O3–Mn–O4	176.5	174.7	N1–Mn–O4	89.3	87.5

of all complexes. The optimized structure of complex 4 is shown in Fig. 3. Table 1 summarizes the most relevant structural parameters together with the crystallographic data.[17] Both solvent models studied gave similar results (see Table SI-I, ESI†).

The coordination around the Mn ion in the optimized complexes may be described as elongated octahedral, with the axial H_2O–Mn–H_2O bond distances (Mn–O 2.29 to 2.33 Å) distinctly longer than the equatorial Mn–O/N bond distances (1.87 to 2.05 Å), a signature of Jahn–Teller distorted Mn^{III} ions.[34] The bond distances and the angles of the optimized structures correlate very well with the data obtained from the crystallographic studies as shown in Table 1. The parameters of all the complexes follow the same trend as shown in the ESI† (Fig. S1 and Table SI-II).

Table 2 summarizes the Mulliken charges and the spin populations of the Mn ion in each complex in both oxidation states. As expected, the spin population is close to the number of unpaired electrons of a high spin d^4 ion (Mn^{3+}) and d^5 ion (Mn^{2+}). On the other hand, since the Mulliken charge does not reflect the formal charge of the metal ion, it is diminished by its delocalization over the ligand. The calculated Mulliken charges are ~0.95 and ~0.75 for the Mn^{3+}/Mn^{2+} central ion.

Spin densities are not altered by the electron donor effect of the substituents, whereas the charge suffers a slight change in accordance with the electron donor or acceptor effect of the substituent.

Table 2 Spin populations and Mulliken charges (in parentheses) for manganese complexes at B3LYP/6-31G**/LANL2DZ/PCM. Q = complex charge, S = spin multiplicity

	Mn^{III}–(X-salpn) Q = +1, S = 5	Mn^{II}–(X-salpn) Q = 0, S = 6
Complex-1	3.87 (0.91)	4.79 (0.69)
Complex-2	3.88 (0.91)	4.78 (0.71)
Complex-3	3.88 (0.94)	4.78 (0.73)
Complex-4	3.88 (0.93)	4.79 (0.73)
Complex-5	3.89 (0.96)	4.79 (0.75)
Complex-6	3.90 (0.97)	4.79 (0.76)
Complex-7	3.90 (0.99)	4.79 (0.78)

Table 3 Experimental and calculated redox potential of complexes 1–7

	E^0 (Mn^{III}/Mn^{II}) (mv) *vs.* Fc/Fc^+		
		E^0_{calc}	
	E^0_{exp}	B3LYP PCM	B3LYP SMD
Complex-1	−714	−1127	−1124
Complex-2	−516	−967	−889
Complex-3	−469	−735	−711
Complex-4	−422	−738	−720
Complex-5	−365	−527	−567
Complex-6	−207	−370	−418
Complex-7	−106	−155	−205

A direct relationship is observed when we compare the redox potential values (Table 3) with the Mulliken charges on the Mn ion of each complex, there exists a direct relationship between them. This is in accordance with the effect over the metallic center due to the substituents in the aromatic rings; thus the electrophilic substituents subtract electronic density from the metallic ion to increase its charge and redox potential. Although there is a correct correlation between the Mulliken charge and the redox potential of the complexes, the fact that the charge variation is very small does not allow us to use it as a parameter for the theoretical predictions.

Redox potentials of the manganese complexes

The calculated redox potentials (E^0_{calc}), as well as the corresponding experimental values (E^0_{exp}), of the complexes are summarized in Table 3. All cited potentials were referenced against the ferrocene/ferrocenium (Fc/Fc^+) couple as suggested by IUPAC.[35] To obtain the redox potentials we performed theoretical calculations at the B3LYP/6-31G**/LANL2DZ level using two solvent models, PCM and SMD. The E^0 of the couple Fc/Fc^+ was calculated using the same protocol.[20] The results obtained with both solvent models are compared in Fig. 4. There is a good linear correlation between the experimental data and calculated values for both models of solvents.

We performed a correlation and regression analysis of both systems. The determined relationship was linear according to the calculated statistics, F_{cal} = 533.4 (PCM) and 1344.3 (SMD) ($F_{crit}(0.05;1;5)$ = 6.6). The ordinate to the origin turned out to be non-significant in the B3LYP/6-31G**/LANL2DZ/PCM calculations. The resulting slope is 0.60 with a standard deviation (SD) of 0.02. When we fit the B3LYP/6-31G**/LANL2DZ/SMD data

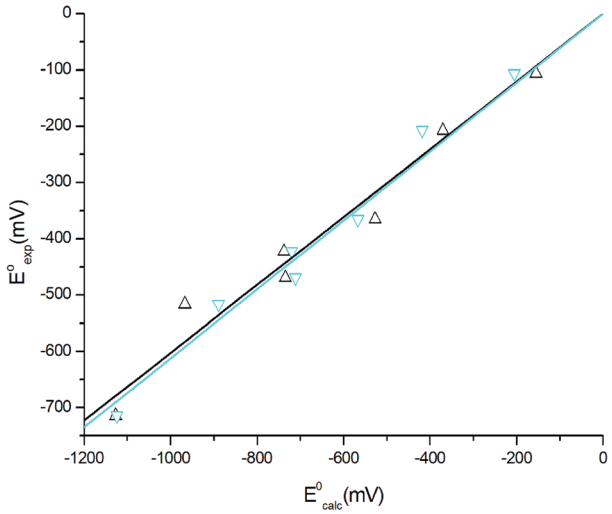

Fig. 4 Plot of calculated and experimental redox potentials for the manganese complexes (*vs.* Fc/Fc^+). Calculations were performed at the B3LYP/6-31G**/LANL2DZ level with PCM in black triangles (Δ) and SMD in cyan triangles (▽). Linear regression of each system is shown in a solid line corresponding to the colour of the symbols.

the slope is 0.66 with a SD of 0.04 and the ordinate is 35.9. The regression coefficient (R) is 0.99 in both cases. The accurate linear fit obtained allows us to use the regression data to predict redox potentials of new manganese complexes.

With the aim of further reducing the computational cost, we decided to perform calculations without considering the effects of the solvent. In Fig. S2 (ESI†), the data of the predictions carried out in a vacuum are shown. It is well observed that this simplification does not provide good results, thus, it is necessary to take into account the effect of the solvent with an implicit model that does not significantly increase the computational cost.

Validation of the model

In order to validate our strategy, we employed two novel complexes synthesized and characterized by our group,[33] to evaluate the performance of the linear regression equation. The redox potential values measured in DMF solvent of complexes 8 and 9 are shown in Table 4.

In both cases the absolute error is ∼50 mV which is lower than the error in the redox potential estimation using single *ab initio* calculations.[20,22] This calculation on complexes obtained in a different laboratory demonstrates the suitability of the strategy, which allows comparison of a series of analogous complexes.

Table 4 Redox potential prediction using the linear regression

	$E^0(Mn^{III}/Mn^{II})$ (mv) *vs.* Fc/Fc^+		
		$E^0_{predict}$	
Complex	E^0_{exp}	B3LYP PCM	B3LYP SMD
Complex-8	−399	−455	−409
Complex-9	−342	−341	−289

Conclusions

In this work, a strategy was applied to predict redox potentials of a family of manganese complexes through computational chemistry calculations. We studied the electronic properties of a series of mononuclear manganese complexes. Through a thermodynamic cycle we were able to estimate the redox potential values of the complexes and we could correlate them with the experimental data. An excellent correlation was found between experimental and theoretical data that correctly fit through a linear regression. This relationship is important to design new complexes with a desired redox potential. The model developed successfully predicted the E^0 of two complexes synthesized in our laboratory demonstrating the aptness of the strategy.

In this way, using a low-cost computational method for calculating redox potentials of transition metal complexes, researchers may facilitate the rational design of biomimetic complexes optimizing resources.

Conflicts of interest

The authors declare no conflicts of interest.

Acknowledgements

This research was supported by grants from CONICET and Universidad Nacional de Rosario to V. A. D., S. S. and D. M. M., all three are staff members of CONICET. J. L. P and S. I. D. have received fellowships from CONICET. The results present in this work were obtained using the resources of the Computer Center of CCT-Rosario, member of the National System of High Performance Computing (SNCAD, MincyT-Argentina).

References

1 *Mechanistic Bioinorganic Chemistry*, ed. H. H. Thorp and V. L. Pecoraro, American Chemical Society, New York, 1995.
2 I. Pálinkó, in *Inorganic Biochemistry Research Progress*, ed. J. G. Hughes and A. J. Robinson, Nova Science Publishers, New York, 2008, pp. 282–303.
3 O. Iranzo, *Bioorg. Chem.*, 2011, **39**, 73–87.
4 C. Muscoli, S. Cuzzocrea, D. P. Riley, J. L. Zweier, C. Thiemermann, Z.-Q. Wang and D. Salvemini, *Br. J. Pharmacol.*, 2003, **140**, 445–460.
5 R. Hage and A. Lienke, *J. Mol. Catal. A: Chem.*, 2006, **251**, 150–158.
6 J. F. Larrow, E. N. Jacobsen, Y. Gao, Y. Hong, X. Nie and C. M. Zepp, *J. Org. Chem.*, 1994, **59**, 1939–1942.
7 D. P. Riley, S. L. Henke, P. J. Lennon, R. H. Weiss, W. L. Neumann, J. Willie, J. Rivers, K. W. Aston, K. R. Sample, H. Rahman, C.-S. Ling, J.-J. Shieh, D. H. Busch and W. Szulbinski, *Inorg. Chem.*, 1996, **35**, 5213–5231.
8 V. Daier, D. Moreno, C. Duhayon, J. Tuchagues and S. Signorella, *Eur. J. Inorg. Chem.*, 2010, 965–974.

9 D. Moreno, V. Daier, C. Palopoli, J.-P. Tuchagues and S. Signorella, *J. Inorg. Biochem.*, 2010, **104**, 496–502.
10 I. Batinić-Haberle, I. Spasojević, R. D. Stevens, P. Hambright, P. Neta, A. Okado-Matsumoto and I. Fridovich, *Dalton Trans.*, 2004, 1696–1702.
11 I. Batinić-Haberle, I. Spasojević, R. D. Stevens, B. Bondurant, A. Okado-Matsumoto, I. Fridovich, Ž. Vujašković and M. W. Dewhirst, *Dalton Trans.*, 2006, 617–624.
12 U. P. Singh, R. K. Singh, Y. Isogai and Y. Shiro, *Int. J. Pept. Res. Ther.*, 2006, **12**, 379–385.
13 S. Signorella, C. Palopoli and G. Ledesma, *Coord. Chem. Rev.*, 2018, **365**, 75–102.
14 P. G. Cozzi, *Chem. Soc. Rev.*, 2004, **33**, 410–421.
15 A. Erxleben, *Inorg. Chim. Acta*, 2018, **472**, 40–57.
16 D. Moreno, V. Daier, C. Palopoli, J.-P. Tuchagues and S. Signorella, *J. Inorg. Biochem.*, 2010, **104**, 496–502.
17 M. Maneiro, M. Bermejo, A. Sousa, M. Fondo, A. González, A. Sousa-Pedrares and C. A. McAuliffe, *Polyhedron*, 2000, **19**, 47–54.
18 C. J. Cramer and D. G. Truhlar, *Phys. Chem. Chem. Phys.*, 2009, **11**, 10757.
19 J. Ye, R. C. Cammarota, J. Xie, M. V. Vollmer, D. G. Truhlar, C. J. Cramer, C. C. Lu and L. Gagliardi, *ACS Catal.*, 2018, **8**, 4955–4968.
20 S. J. Konezny, M. D. Doherty, O. R. Luca, R. H. Crabtree, G. L. Soloveichik and V. S. Batista, *J. Phys. Chem. C*, 2012, **116**, 6349–6356.
21 L. E. Roy, E. R. Batista and P. J. Hay, *Inorg. Chem.*, 2008, **47**, 9228–9237.
22 L. Yan, Y. Lu and X. Li, *Phys. Chem. Chem. Phys.*, 2016, **18**, 5529–5536.
23 A. D. Becke, *J. Chem. Phys.*, 1993, **98**, 5648–5652.
24 M. J. Frisch, G. W. Trucks, H. B. Schlegel, G. E. Scuseria, M. A. Robb, J. R. Cheeseman, G. Scalmani, V. Barone, G. A. Petersson, H. Nakatsuji, X. Li, M. Caricato, A. Marenich, J. Bloino, B. G. Janesko, R. Gomperts, B. Mennucci, H. P. Hratchian, J. V. Ortiz, A. F. Izmaylov, J. L. Sonnenberg, D. Williams-Young, F. Ding, F. Lipparini, F. Egidi, J. Goings, B. Peng, A. Petrone, T. Henderson, D. Ranasinghe, V. G. Zakrzewski, J. Gao, N. Rega, G. Zheng, W. Liang, M. Hada, M. Ehara, K. Toyota, R. Fukuda, J. Hasegawa, M. Ishida, T. Nakajima, Y. Honda, O. Kitao, H. Nakai, T. Vreven, K. Throssell, J. A. Montgomery, Jr., J. E. Peralta, F. Ogliaro, M. Bearpark, J. J. Heyd, E. Brothers, K. N. Kudin, V. N. Staroverov, T. Keith, R. Kobayashi, J. Normand, K. Raghavachari, A. Rendell, J. C. Burant, S. S. Iyengar, J. Tomasi, M. Cossi, J. M. Millam, M. Klene, C. Adamo, R. Cammi, J. W. Ochterski, R. L. Martin, K. Morokuma, O. Farkas, J. B. Foresman and D. J. Fox, *Gaussian 09*, Gaussian Inc., Wallingford, CT, 2009.
25 R.-Z. Liao, M. D. Kärkäs, B.-L. Lee, B. Åkermark and P. E. M. Siegbahn, *Inorg. Chem.*, 2015, **54**, 342–351.
26 K. Miyagawa, K. Komi, J. Ohnari, S. Maruyama, S. Yamanaka, T. Saito, T. Kawakami, K. Yamaguchi and M. Okumura, *Polyhedron*, 2017, **136**, 102–109.
27 E. Rossini and E.-W. Knapp, *Coord. Chem. Rev.*, 2017, **345**, 16–30.
28 E. M. Sproviero, *J. Inorg. Biochem.*, 2017, **171**, 52–66.
29 G. A. Petersson and M. A. Al-Laham, *J. Chem. Phys.*, 1991, **94**, 6081–6090.
30 P. J. Hay and W. R. Wadt, *J. Chem. Phys.*, 1985, **82**, 270–283.
31 J. Tomasi, B. Mennucci and E. Cancès, *J. Mol. Struct. THEOCHEM*, 1999, **464**, 211–226.
32 A. V. Marenich, C. J. Cramer and D. G. Truhlar, *J. Phys. Chem. B*, 2009, **113**, 6378–6396.
33 C. Palopoli, G. Gómez, A. Foi, F. Doctorovich, S. Mallet-Ladeira, C. Hureau and S. Signorella, *J. Inorg. Biochem.*, 2017, **167**, 49–59.
34 V. Solís, C. Palopoli, V. Daier, E. Rivière, F. Collin, D. M. Moreno, C. Hureau and S. Signorella, *J. Inorg. Biochem.*, 2018, **182**, 29–36.
35 G. Gritzner and J. Kuta, *Pure Appl. Chem.*, 1984, **56**, 461–466.